

Elimination of zero-activity regions in dynamic laser speckle coating drying experiments

E. Stoykova^{1,2,*}, T. Nikova¹, B. Ivanov¹, Y-M. Kim², H-J. Kang²

1Institute for Optical Materials and Technologies "Acad. J. Malinowski", Bulgarian Academy of Sciences, "Acad. G. Bonchev" str. Bl. 109, 1113 Sofia, Bulgaria

2Korea Electronics Technology Institute, 8 Floor, 11, World cup buk-ro 54-gil, Mapo-gu, Seoul, Korea

Received October 10, 2016; Revised November 14, 2016

Dynamic laser speckle method is a useful approach for monitoring the speed of processes by statistical processing of speckle patterns formed on the surface of diffusely reflecting object at laser illumination. The most popular algorithms are the intensity-based pointwise algorithms which rely on capture of correlated in time speckle patterns. These algorithms fail at non-uniform illumination and require pointwise normalization to produce correct results. The normalized processing encounters difficulties in detection of non-varying regions on the object surface. The paper proposes usage of a specially designed estimator to eliminate these regions.

Keywords: dynamic speckle, intensity-based algorithms, pointwise processing,

INTRODUCTION

Dynamic laser speckle method enables monitoring of processes by detection of speckle patterns formed on the surface of diffusely reflecting objects at coherent light illumination [1,2]. The speckle patterns reflect the microscopic changes on the object surface and thus provide a very sensitive tool for indicating changes. The method is effective for non-destructive testing of industrial samples as drying of paints or coatings, biomedical applications and food quality assessment [3-5]. Dynamic speckle metrology has been pushed forward by advances in modern optical sensors and computers that make possible pointwise processing and characterization of the monitored process by a two-dimensional (2D) distribution of a given statistical parameter related to its speed. This map is called an activity map and allows for differentiation of regions with slow or fast changes of speckle patterns on the object surface [6]. The main advantage of dynamic speckle technique is the simple experimental means of performing the measurement. The main disadvantage is that the statistical processing is vulnerable to non-uniform illumination or varying reflectivity across the object due to the signal-dependent nature of speckle fluctuations. To

overcome this drawback, pointwise normalization is applied to the statistical estimates of activity [7]. Normalization, however, fails in the regions with almost zero activity and gives an erroneous result by indicating activity much greater than the existing really. The goal of this paper is to develop reliable procedure for detecting zero-activity regions by combining normalized and non-normalized processing. Experimental verification of the developed approach is done by processing paint coating drying.

POINTWISE CHARACTERIZATION

Generally speaking, capture of 2D dynamic speckle patterns by a CCD camera allows to build a 2D spatial distribution of some measure which characterizes activity related to different spatial regions of the sample under study for a given time interval. For the purpose, a series of N frames is acquired for the observation time T . Thus, the 8-bit encoded and sampled intensities, $I_{kl,n} = I(k\delta x, l\delta y; n\Delta t), n = 1, 2, \dots, N$, which correspond to a given pixel $(k\delta x, l\delta y)$ in the recorded N frames, form a time sequence (Fig. 1). Here $(\delta x, \delta y)$ are the sampling intervals along the N_x rows and N_y columns of the captured image and $\Delta t = T/N$ is the time interval between two consecutive images. The estimate of the chosen statistical measure is found at all points $(k\delta x, l\delta y)$, $k = 1, 2, \dots, N_x, l = 1, 2, \dots, N_y$, after

* To whom all correspondence should be sent:
E-mail: elena.stoykova@gmail.com

averaging over the formed time sequences. The obtained 2D distribution of the estimate corresponds to T and hence it gives localized in space and not localized in time estimate of sample activity. The time interval T should cover several radii of the temporal correlation function of intensity fluctuations caused by the undergoing activity within the sample to have enough data for a reliable estimate.

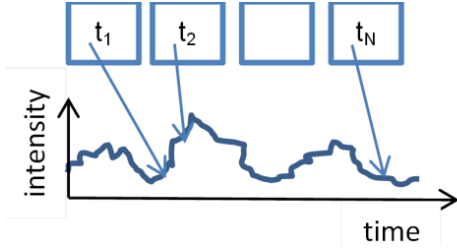


Fig. 1. Capture of a time sequence of 2D speckled patterns

A measure based on evaluation of the temporal structure function (TSF) at $(k\delta x, l\delta y)$, $k = 1, 2, \dots, N_x, l = 1, 2, \dots, N_y$ yields localized in time 2D descriptions of activity for time lags $\tau = m\Delta t, m = 1, 2, \dots, M$ which correspond to the averaging interval T :

$$\hat{S}(k, l, m) = \frac{1}{(N-m)} \sum_{n=0}^N (I_{kl,n} - I_{kl,n+m})^2 \quad (1)$$

We can also describe the time fluctuations by using a normalized temporal structure function (NTSF). The estimate of the NTSF for each point $(k\delta x, l\delta y)$ is built as follows:

$$\hat{S}_{norm}(k, l, m) = \frac{1}{(N-m)} \frac{1}{\bar{v}(k, l)} \sum_{n=0}^N (I_{kl,n} - I_{kl,n+m})^2 \quad (2)$$

$$\bar{v}(k, l) = \frac{1}{N} \sum_{n=1}^N (I_{kl,n} - \bar{I}_{kl})^2, \quad \bar{I}_{kl} = \frac{1}{N} \sum_{n=1}^N I_{kl,n} \quad (3)$$

where $\bar{v}(k, l)$ and \bar{I}_{kl} are the estimates of the variance and the mean intensity that are calculated at the spatial point $(k\delta x, l\delta y)$. For a time lag $\tau = m\Delta t$ the estimates $\hat{S}_{norm}(k, l, m)$ and $\hat{S}(k, l, m)$ are given by 2D spatial distributions where the small values of \hat{S}_{norm} or \hat{S} correspond to large correlation and hence indicate lower activity within the sample and vice versa. Theoretically the NTSF varies from 0 to 1.

EXPERIMENTAL

To check the efficiency of correlation-based algorithms to locate different activity regions we performed measurements with the test object in Fig. 2. The surface of the object was covered with concentric grooves of varying depth and width. A coin was placed in the circular hollow region at the centre of the object. The object was covered with a nail polish, whose drying produced a dynamic speckle. The correlation of data in the regions corresponding to the grooves is larger in comparison to those of the flat surface due to the larger quantity of the nail polish there. The same is valid to some extent for the different parts of the coin due to its varying relief. For the experiment, only the lower half of the object was covered with the nail polish. Illumination of the object was done with a He-Ne laser. The acquisition of speckle patterns was made at a rate of $\Delta t = 500$ ms between the frames. The captured images size was 580×780 pixels.

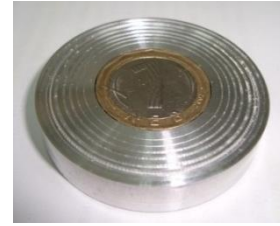


Fig. 2. Test object.

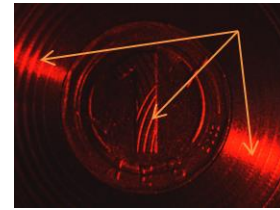


Fig. 3. Image acquired by the CCD camera (the arrows show unusable regions).

We processed 170 speckle patterns with the NTSF and TSF algorithms. An exemplary captured image is shown in Fig. 3. As it is seen, the object surface has non-uniform reflectivity. The arrows indicate the regions of specular reflection for which the recorded intensity everywhere reaches 255 gray levels, and moreover it keeps this value for the whole series. Obviously, information is lost in these regions, and the data in them should be discarded. We excluded the rightmost part of the recorded images due to the large non-informative area and chose to process the data in the region with size

500×500 pixels with a bias of 50 rows and 0 columns. The results obtained for the NTSF are shown in Fig. 4. The light regions correspond to lower correlation and hence to higher activity. Registration of activity is expected for the lower half of the object. The NTSF in the upper part should remain constant. We see that the data in the narrow grooves on center of the coin should be also discarded. The obtained NTSF maps clearly show regions of different activity. We see higher correlation in the region of the concentric grooves as well as on the surface of the coin up to the lag $20\Delta t$; at greater lags there is no correlation between the recorded images. However, the NTSF estimate does not reflect properly the lack of activity in the upper half of the object. Theoretically the NTSF in this region should be close to zero everywhere. The averaged NTSF distribution is uniform indeed, but the mean value of the NTSF in this region is constantly decreasing and is much higher than zero. The inaccuracy of the estimate is due to the short length (170 images) of the series used for calculations. We may conclude that the algorithms with the normalization when applied to short time-series fail to indicate clearly the zero-activity regions. The processing should pick-up automatically and correctly these regions.

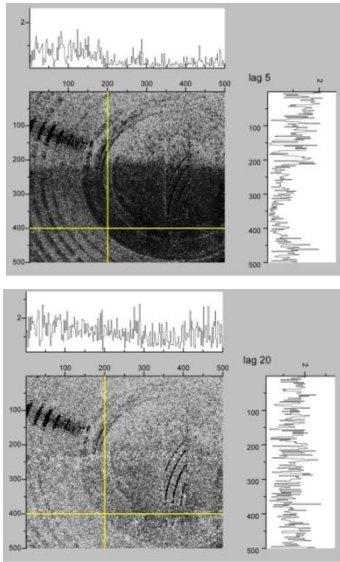


Fig. 4. NTSF at time lags $\tau = 5\Delta t$ and $\tau = 20\Delta t$ (the grey scale varies from 0 to 2.5).

The SF without normalization also clearly separates the upper and the lower object parts (Fig. 5). The mean square of the difference between the intensities is much higher in the lower half of the TSF map. One should take in mind, however, that the value of the mean square rapidly increases with

the reflective property of the object. For example, reflectivity in the grooves region and the coin is higher than on the flat object sections. Dependence of the TSF on the reflectivity across the object renders difficult obtaining information about the activity time scale in different regions of the object. Nevertheless, we could use these function to cut out the zero activity regions

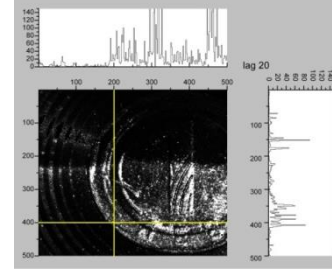


Fig. 5. TSF at a time lag $20\Delta t$ (the grey scale varies from 0 to 140).

To locate the regions with almost zero activity, we introduce the following estimator:

$$\hat{P}(k,l,m) = \frac{1}{(N-m)} \frac{1}{\hat{M}_{sq}(k,l)} \sum_{n=1}^N (I_{kl,n} - I_{kl,n+m})^2 \quad (4)$$

where $\hat{M}_{sq} = \frac{1}{N} \sum_n I_{kl,n}^2$ is the estimate of the mean square.

To clarify $\hat{P}(k,l,m)$ let us suppose that the intensity fluctuations have the same mean value and variance across the image and that the variation in time is a stationary process. Therefore, we may write for any point $I(n\Delta t + m\Delta t) = I(n\Delta t) + \delta I(m\Delta t)$, where $\delta I(m\Delta t)$ is the rise of intensity. Then

$$\langle \hat{P}(m) \rangle \approx \frac{1}{\mathfrak{S}} \{ 2\mathfrak{S} - 2[\mathfrak{S} + \langle I(n\Delta t)\delta I(n\Delta t) \rangle] \} \quad (5)$$

where $\mathfrak{S} = \langle I^2(n\Delta t) \rangle = \langle I^2(n\Delta t + m\Delta t) \rangle$ is the mean square. It is clearly seen from the above expression that the estimator $\hat{P}(k,l,m)$ is zero when $\delta I(m\Delta t) = 0$. When the intensities $I(n\Delta t)$ and $I(n\Delta t + m\Delta t)$ are not correlated, the estimator becomes

$$\langle \hat{P}(m) \rangle \approx 2 \left[1 - \frac{\bar{I}^2}{\mathfrak{S}} \right] = 2 \left[1 - \frac{\bar{I}^2}{\nu + \bar{I}^2} \right] = \frac{2}{1 + (\sigma_I / \bar{I})^2} \quad (6)$$

where $\sigma_I = \sqrt{\nu}$ is the standard deviation of the fluctuations and ν is their variance. We see that the higher the fluctuations, the higher is the value of $\hat{P}(k,l,m)$. At $\sigma_I = \bar{I}$, which is the case of the fully developed speckle [1], the estimator value is one.

We propose to use the introduced estimator in the following way:

1) to calculate $\hat{P}(k,l,m)$ for a comparatively large time lag which guarantees detection of variations in the recorded speckle pattern;

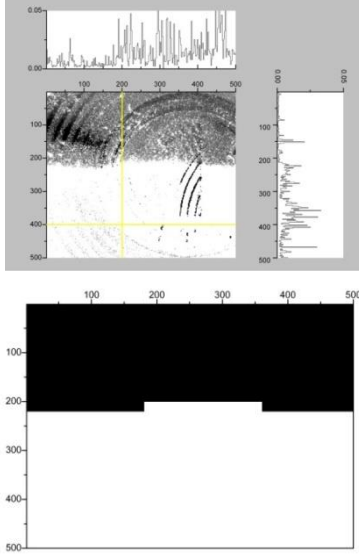


Fig. 6. Distribution of the estimator $\hat{P}(k,l,m)$ at $m = 30$ (top) and the calculated mask (bottom).

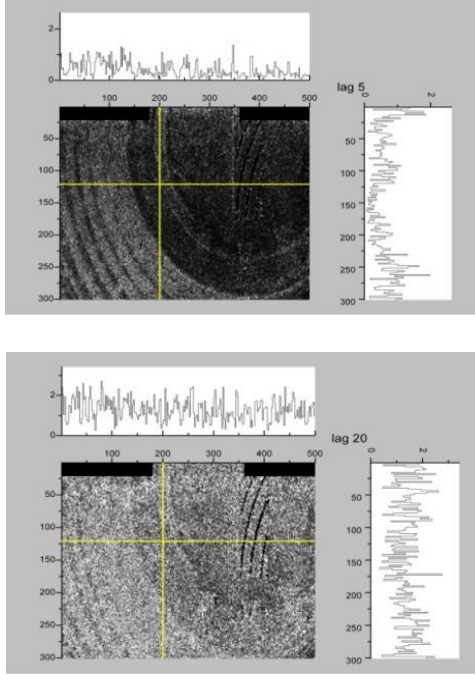


Fig. 7. NTSF at time lags $\tau = 5\Delta t$ and $\tau = 20\Delta t$, multiplied by the mask (the grey scale is from 0 to 2.5).

2) to set a threshold value close to zero, e.g. $\varepsilon = 0.002$, and to create the mask:

$$M(k,l) = \begin{cases} 0 & \text{if } \hat{P}(k,l,m) < \varepsilon \\ 1 & \text{if } \hat{P}(k,l,m) \geq \varepsilon \end{cases} \quad (7)$$

3) to eliminate the spurious fluctuations in $\hat{P}(k,l,m)$ that may lead to non-connected single points in the mask, the mask is filtered with a sliding window of size 10×10 ; if the sum of the values in the window exceeds 60, a unity value is attached to all values inside the window;

4) the NTSF distributions are multiplied by the mask to remove the regions of zero activity.

Fig. 6 depicts the distribution of $\hat{P}(k,l,m)$ at $m = 30$, and the mask derived from it. Fig. 7 shows the distributions of the NTSF multiplied by the mask. We obtain the highest correlation of fluctuations on the surface of the coin. The correlation is higher in the grooves than in the flat object sections. As it should be expected, the correlation disappears first for the thinner grooves. They are undistinguishable from the flat sections at time lags 20 and 40 whereas the thicker grooves are still seen.

CONCLUSIONS

In summary, we developed a dynamic speckle approach based on combined usage of normalized and non-normalized processing for elimination of zero-activity regions from activity maps obtained for the normalized correlation-based algorithms. The problem with erroneous detection of activity in these regions arises from small value of the variance and inaccurate determination of its estimates at short lengths of the temporal sequences formed from the acquired speckle images. Efficiency of the proposed approach was confirmed by processing a test object half coated with a polyester paint. The developed algorithm formed automatically a mask to preserve only regions with non-zero activity.

Acknowledgment: This paper is supported by the Ministry of Science, ICT, and Future Planning (MSIP) (Cross-Ministry Giga KOREA Project).

REFERENCES

1. J. Goodman, Statistical Optics, Wiley – Interscience, 2000.
2. H. Rabal, R. Braga, Dynamic laser speckle and applications, CRC Press, Boca Raton, 2009.
3. B. Zheng, C. Pleass, and C. Ih, *Appl. Opt.*, **33**(2), 231-237 (1994).
4. R. Arizaga, N. Cap, H. Rabal, and M. Trivi, *Opt. Eng.*, **41**, 287 (2002).
5. A. Saúde, F. de Menezes, P. Freitas, G. Rabelo, and R. Braga, *J. Opt. Soc. Am. A*, **29**, 1648 (2012).

6. E. Stoykova, D. Nazarova, N. Berberova, and A. Gotchev, *Opt. Express*, **23**, 25128 (2015). 7. E. Stoykova, B. Ivanov, and T. Nikova, *Opt. Lett.*, **39**, 115 (2014).

ОТСТРАНЯВАНЕ НА ОБЛАСТИТЕ С НУЛЕВА АКТИВНОСТ ПРИ ДИНАМИЧЕН СПЕКЪЛ АНАЛИЗ НА СЪХНЕНЕ НА ПОКРИТИЯ

Е. Стойкова^{1,2}, Т. Никова¹, Б. Иванов¹, Й.М. Ким², Х.Дж. Канг²

*1Институт по оптически материали и технологии "Акад. Й. Малиновски", Българска Академия на науките,
ул. "Акад. Г. Бончев", бл. 109, 1113 София, България*

2Корейски институт по електронни технологии, 8 етаж, 11, Уорлд-кап бук-ро, 54-джил, Мапо-гу, Сеул, Корея

Постъпила на 10 октомври 2016 г.; коригирана на 14 ноември, 2016 г.

(Резюме)

Динамичният спекъл метод е полезен подход за мониторинг на скоростта на протичане на процеси чрез статистическа обработка на спекъл картините, образиващи се върху повърхността на дифузно отразяващи обекти при осветяване с лазер. Най-популярни са интензитетно-базираните алгоритми, които изискват запис на корелирани във времето спекъл изображения. Тези алгоритми не са ефективни при неравномерно осветяване и се налага провеждането на поточково нормиране за постигане на коректни резултати. Обработката с поточково нормиране среща трудности при детектирането на области без промяна върху повърхността на обекта. В статията се предлага използването на специално изградена оценка за отстраняване на тези области.